Volume 2, Number 2, pp. 42-53, 2000.

■ Home Current Issue Table of Contents

Mathematical Model of the Electrical Activity of Ventricular Cell: Regional Differences and Propagation

Z. Li, H. Zhang, A.V. Holden, and C.H. Orchard

School of Biomedical Sciences, University of Leeds, LS2 9JT, UK

Correspondence: Lizzie@cbiol.leeds.ac.uk

Abstract. The characteristics of electrical activity of isolated cells from guinea-pig ventricular wall show regional differences. These regional differences are assumed to be results of regional differences in membrane ionic current densities. Mathematical models incorporating the experimental data of variable ionic current densities are able to reproduce the regional differences in action potentials. In one-dimensional model of intact ventricular tissue, electrotonic interactions between cells reduced regional differences shown in isolated single cells.

Keywords: Guinea-pig, Ventricular myocardium, Regional differences.

Introduction

In recent years, extensive studies have found that there are regional differences in the electrical activities of mammalian ventricular myocytes. Electrical activities of cells isolated from sub-epicardial and sub-endocardial myocardium show different characteristics. Such regional differences are species dependent. In the heart of canine [1, 2, 3], feline [4, 5], rabbit [6], rat [7, 8], and human [9, 10] action potentials of endocardial ventricular cells have a longer action potential duration (APD), higher amplitude (AM), and more negative resting potential (RP) than those of epicardial cells. In some species, electrical activities of epicardial cells have a spike-and-dome morphology, which is absent in endocardial cells. The mechanisms underling such regional differences are unclear. It has been assumed that such regional differences may result in the variability of the membrane ionic current densities. For example, experimental data have shown that in the ventricle of canine's heart, epicardial cells have a larger ionic current density and a faster speed of inactivation of outward transit current Ito [2]. The difference in the morphology of action potential between epicardial cells and endocardial cell may be due to the regional difference of Ito: both the current density and gating speed. Experimental data have also shown that there is a large difference in the ionic current densities of slowly and rapidly activated delayed rectifier potassium current IKr and I_{Ks} [2], and their associated channel kinetics between epi- and endo-cardial ventricle cells.

Regional differences in action potential durations of epi- and endo-cardial ventricle cells may be due to the cooperative effect of regional differences in I_{Kr} , I_{Ks} and I_{to} [11].

In guinea-pig ventricle, unlike those of other species, electrical activities of cells isolated from different regions of ventricular wall show no significant difference in action potential configuration, such as the spike-and-dome morphology, and the resting potential. However, it has been found that the action potential durations at 50% (APD $_{50}$) and 90% (APD $_{90}$) repolarization are significantly shorter in subepicardial myocytes than in subendocardial myocytes [12, 13, 14]. In other species, I_{to} contributed to the differences in the action potential configuration. In guinea-pig ventricular cells, experiments have failed to find evidence for the existence of I_{to} [15, 16, 17]. The difference in APD is assumed to be mainly due to the relative densities of I_{Kr} and I_{Ks} , and their associated channel kinetics [13, 14]. To test this hypothesis, we constructed mathematical models for endo- and epi-cardial ventricular cells of guinea-pig heart. These models incorporate the experimental data of regional differences of ionic current densities. The model action potentials show the same characteristics of action potentials and their regional differences as those recorded from cells isolated from epi- and endo-cardial ventricular cells of guinea-pig heart.

In intact ventricle, the recorded electrical activity from different region did not show the same remarkable regional differences as seen in isolated cells [18]. Such a significant quantitative difference has raised a question, whether or not regional differences shown in the electrical activity of epi- and endo-cardial ventricle cells is due to the intrinsic properties of cells, or due to damage of cells in the process of isolation during experiments? If it is an intrinsic property of cells, what is the mechanism underlying such an apparent disagreement between the data obtained from isolated cells and intact ventricle? In other words, what is the reason for the regional difference to disappear in the intact ventricle? We approach this question computationally. Here we constructed a one-dimensional model of a transmural string of ventricular wall, extending from the endo- to epicardium. The one-dimensional model incorporates the heterogeneity in the electrical activity of ventricular cell. It is shown that, due to the electrotonic interactions, the regional differences in action potential characteristics recorded from different sites are reduced.

Methods - Model development

Single cell models

Models of electrical activity of epi- and endo-ventricular cells of guinea-pig heart are based on modifications of a standard model of electrical activity of guinea-pig ventricular cell [19, 20]. The models consist of a set of ordinary differential equations derived from the results of extensive electrophysiological experiments on guinea-pig ventricular myocytes. It represents voltage-dependent ionic currents, pump/exchanger currents, time dependent changes in intracellular and extracellular ionic concentrations, and storage and release of Ca²⁺ by intracellular organelles. In the models we incorporated the published experimental data of Bryant et al. [14] on the ionic current densities measured in isolated guinea-pig ventricular endocardial and epicardial cells. The magnitudes of the Na⁺-K⁺ pump and exchange currents were also modified. The equations, together with the parameter values, are listed in the Appendix.

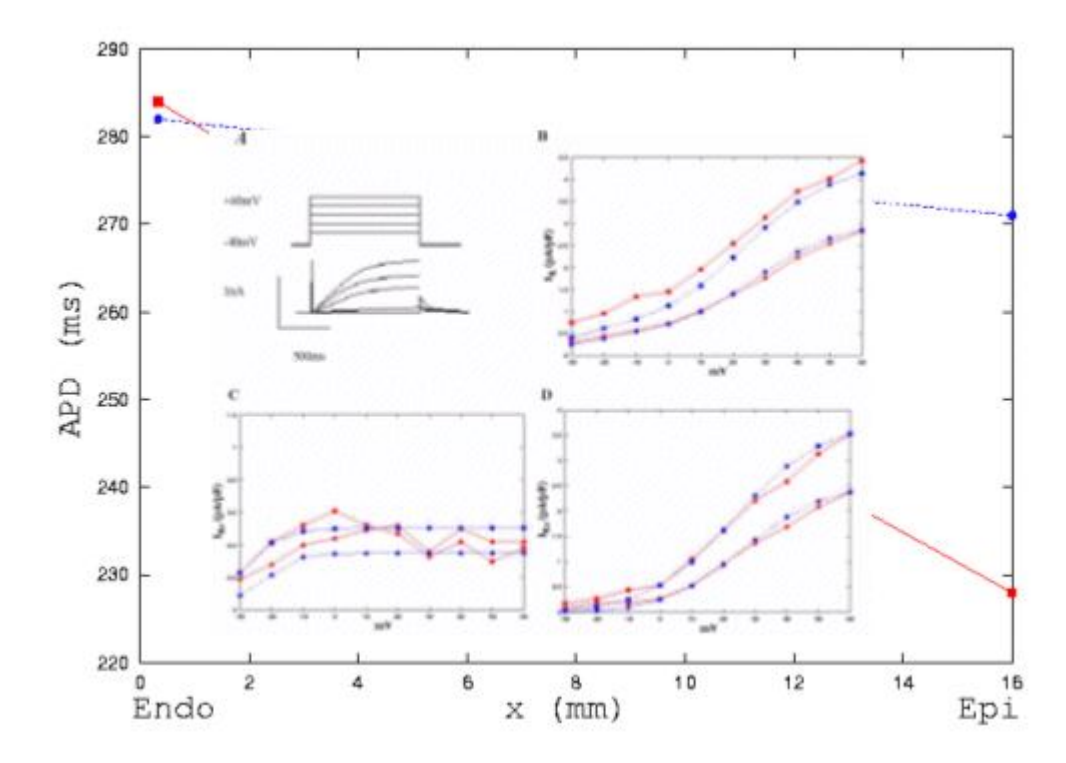


Figure 1: Delayed rectifier tail current densities in endo- (circles) and epicardial (squares) cells of guinea-pig ventricle: experimental data (red lines) [14] and computed results (blue lines). Panel A, shows am example of the protocol used to elicit time-dependent and tail currents, which were elicited upon repolarisation to -40 mV after a 1 s step depolarisation to -20 mV, 0 mV, +20 mV, +40 mV, and +60 mV from a holding potential of -40 mV. Panel B, C and D, current-voltage relationship curves for I_K , I_{Kr} and I_{Ks} tail currents.

Based on the experimental data of Bryant et al. [14], we modified the kinetics of I_{Kr} and I_{Ks} , and also incorporated their regional dependent ionic current densities in our epi- and endoventricular models. To do that, we simulated voltage clamp experiment with a same protocol as used in experiments. The current-voltage relationship curves were simulated to fit the experimental data by choosing value of the ionic conductance of G_{Kr1} , G_{Kr2} (fast and slow components of I_{Kr}) and G_{Ks} and the rates of activation and inactivation of I_{Kr} and I_{Ks} for endo- and epicardial ventricular cells.

Figure 1 shows the simulation of the voltage clamp experiment, and comparison with the experimental data of Bryant et al. [14]. In Figure 1A, the top panel shows the voltage clamp protocol. The cell membrane potential is clamped from a holding potential of -40 mV to +60 mV for 1 s duration. The bottom panel shows the time trace of I_K . In figure 1B, we plotted the I-V relationship of I_K . The current density of I_K is estimated by the peak tail current at the end of the test pulse. In the figure, filled square with solid line represents the data computed from the epi-cardial cell mode, filled circle with solid line represents the computed data from endo-cardial model; filled square with dash line represents the mean data obtained from epicardial cells, filled circle with dash line represents the mean data obtained from endocardial cells. Our computed data fitted quite well with the experimental data.

Figure 1C plots the I-V relationship of I_{Kr} , and comparison with experimental data. In the figure, solid square with solid line is the data from epicardial cell model, filled circle with solid line is the data from endocardial cell model. The computed data for both epi- and endocardial cells are within the experimental range of the mean data obtained from epi-(solid square with dashed line) and endo-cardial cells (solid circle with dashed.).

In Figure 1D, we plotted the computed I-V relationship of I_{Ks} , and comparison with experimental data. Once again, solid squares represent the data from epicardial cell model (with solid line) and the mean data from epicardial cells (with dashed line); solid circles represents the data from endocardial cell model (with solid line) and the mean data from endocardial cells. For both the epi- and endocardial cell models, the computed data are consistent with the experimental data.

Table 1 lists the experimental data (mean + S.E.M.) of ionic current densities of I_K , $I_{K,r}$ and $I_{K,s}$ obtained from n cells isolated from epi-cardial and endo-cardial ventricular cell (n changes from 9 to 12). Our model generated data are also listed. The model generated data are within the range of experimental data.

TABLE 1: Regional differences in the delayed rectifier current in guinea-pig ventricular myocytes between experimental data and our modelling result [14]:

		Experimental data		Our modeling result	
		Endo	Epi	Endo	Epi
I _K at 0 mV	(pApF ⁻¹)	0.73±0.08	1.21±0.13	0.71	1,13
I _K at 60 mV	$(pApF^{-1})$	2.74±0.27	3.90±0.41	2.85	4.13
I _{Ks} at 0 mV	(pApF ⁻¹)	0.29±0.07	0,60±0.12	0.25	0.54
I _{Ks} at 60 mV	(pApF-1)	2.29±0.33	3.52±0.41	2.38	3.53
I _{Kr} at 0 mV	(pApF ⁻¹)	0.44±0.07	0.61±0.08	0.35	0.50

 I_K is tail currents elicited upon repolarisation to -40 mV after 1s step depolarisation to either -30 mV or +60 mV. I_K is tail current density measured in normal Tyrode. I_{Ks} = defetilide-insensitive tail current density and I_{Kr} = defetilide-sensitive tail current density.

One dimensional model incorporating heterogeneity

A one-dimensional model of a transmural string of ventricular wall takes the form of partial differential equation. In the model we incorporated the heterogeneities of ionic current densities. We assumed that the length of string is 16 mm. In the string, cell capacitance changes linearly from 132 pF at the epicardial to 142 at the endocardial end. The ionic current densities are linear functions of cell capacitance. Electrotonic interactions between cells are through diffusive interactions of membrane potentials. The model takes the form:

$$V(x,t) / \partial t = -I_{tot}(x,t) / C_m + V^2 DV(x,t)$$
 (1)

in which, V(x,t) is the membrane potential of a node at x distance from the end of epicardium, D is the diffusion coefficient for V, ∇^2 is the Laplacian operator. In numerical simulation, the partial differential equation is solved by a 3-node Laplacian operator, and a time step dt of 0.1 ms, space step dx of 0.32 mm. The diffusion coefficient D was set to 256 mm²s⁻¹ to give a conduction velocity of 0.3 ms⁻¹.

Results

Simulated action potentials and their regional differences

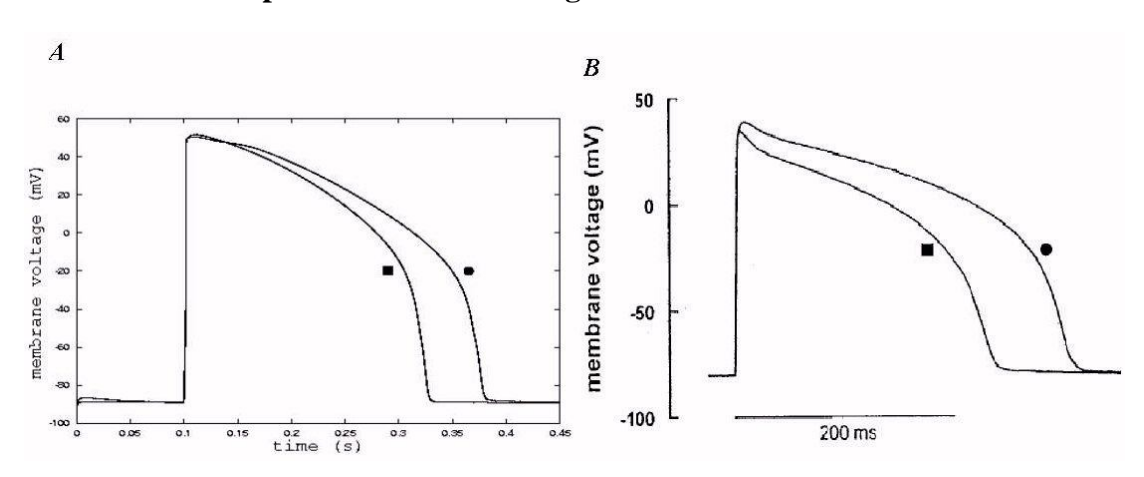


Figure 2: Action potentials of the endo- (circle) and epicardial (square) cells of guineapig ventricle: (A) simulated result (B) experimental data [14]

Figure 2A shows the model generated action potentials of epi- and endo-ventricular cells (circle for endocardial cell; square for epicardial cell) in response to a supra-threshold stimulus. The model action potentials are compared with action potentials recorded from epi-and endo-cardial ventricular cells of guinea pig heart (Figure 2B). In both simulation and experimental recording, action potential of epi-cardial cell has significantly shorter APD than that of endocardial cell. However, there is no difference in resting potential. In simulation, there is no difference in the amplitude of action potentials, however, in experimental recording, there is noticeable difference in the amplitude. Difference in the amplitude may result in other ionic currents involved, such as the sustained background sodium current [14].

Table 2 gives detailed comparison of characteristics of action potentials of epi- and endocardial ventricular cells. In the table, the experimental data are in mean + S.E.M (n changes from 30 to 40) format. From the table we can see that our model generated action potentials of epi- and endo-cardial ventricular cells have the same region characteristics as those recorded experimentally. The model generated action potential duration (APD) is shorter in the epicardial myocytes than in the endocardial myocytes. APD measured at 50% and 90% repolarization were longer in endocardial myocytes than in epicardial myocytes either in the experimental data and computed results: with a stimulation interval of 5000 ms, the action potential duration measured at 50% repolarization (APD₅₀) from the endocardial and epicardial cell models was 261 ms and 198 ms, which are consistent with the experimental results of 250 \pm 12 and 185 \pm 9 ms, and the APD₉₀ was 284 ms and 228 ms, while the experimental results are 292 \pm 12 and 227 \pm 9 ms. There is no significant difference in the simulated AP resting potential and amplitude.

TABLE 2: Regional differences in the characteristics of action potentials of guinea-pig ventricular cells between experimental data [14] and computed results:

	Endocardial myocyte experimental computed		Epicardial myocyte experimental computed	
	data	result	data	result
Resting potential (mV)	-79±1	-86.03	-78±1	-85.96
AP amplitude (mV)	118±1	134.78	113±2	134.75
AP overshoot (mV)	39±1	48.75	35±1	48.79
APD ₅₀ (ms)	250±12	261	185±9	198
APD ₉₀ (ms)	292±12	284	227±9	228

It is known that characteristics of action potential of guinea-pig ventricular cells are rate dependent. If a second action potential is initiated soon after the first, the second action potential in found considerably shorter in action potential duration. Such rate dependence can been illustrated by a restitution curve [21, 22]. Here we investigate a possible regional difference in the rate dependence between epi- and endo-cardial cells, as a result of regional difference in their ionic current densities. In figure 3, we plot the normalized action potential duration against the time interval between two successive stimuli. In the figure, circle represents data computed from epicardial cell model, while square represents data computed from the endocardial cell model. With a slow stimulus rate (a longer time interval), there is no differences. With a high stimulus rate (a small time interval), the difference becomes noticeable.

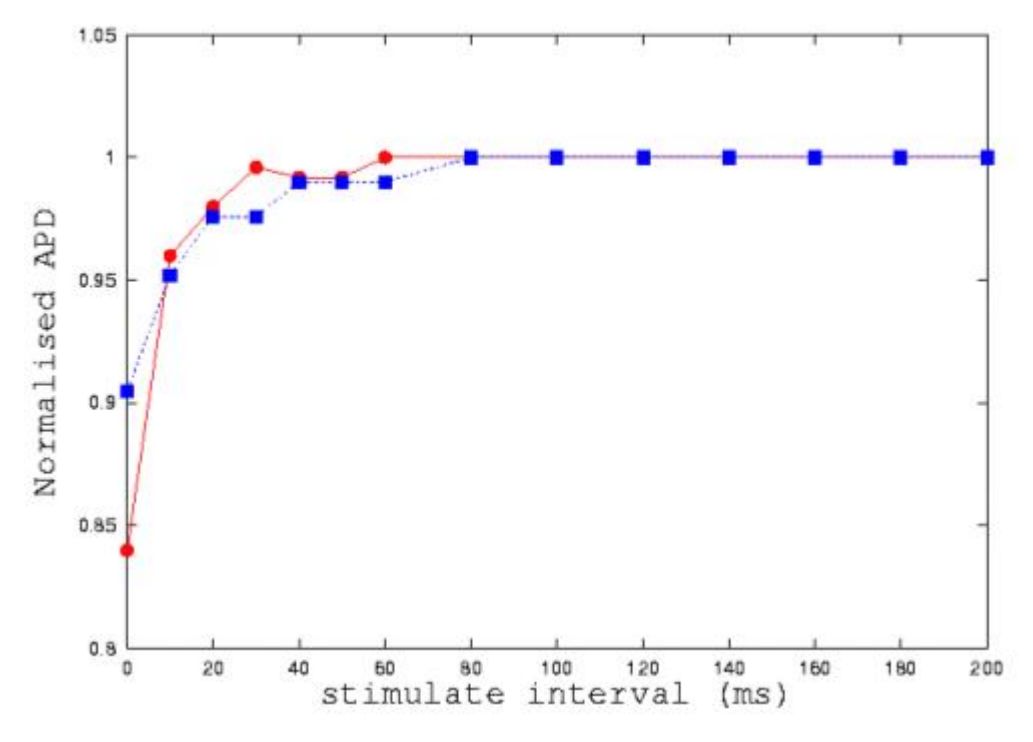


Figure 3: Computer modelling of restitution curves of the endo- (circle) and epicardial (square) cells of guinea-pig ventricle.

Propagation of electrical activity in one-dimensional model

In one dimensional model of a string of transmural ventricular tissue, intrinsic electrical activity of cells along the string show gradient characteristics as shown in Figure 4A. Action potentials from various points along the string are shown. In numerical simulation we set the cell to cell coupling coefficient to zero, and stimulate all cells in the string simultaneously with a supra-threshold. The excited action potential is displaced from top (0 mm: endocardial) to bottom (16 mm: epicardial). From the endocardial to the epicardial end, the action potential duration decreases gradually. The measured APD_{90} was 284 ms and 228 ms from isolated endocardial and epicardial cells. The difference in APD_{90} is significant.

However, when cells are coupled together, the difference in APD_{90} between endocardial and epicardial cells is reduced. This is shown in figure 4B, in which action potentials along the length of string are shown. In this case, a supra-threshold stimulation is applied at the endocardial end. The evoked excitation wave propagates from endocardium to epicardium. Due to the electronic interactions, the regional differences in action potential duration were partly reduced when electrical activity propagating through the heterogenous guinea-pig ventricular wall: the measured APD_{90} was 282 ms at the end of endocardium and 271 ms.

In the simulation shown in figure 4B, although electrotonic interaction reduced the difference in action potential duration between the endocardial and epicardial cells, however, the sequence of depolarisation and repolarisation is consistent with experimental observations. In the figure, we can see the depolarisation starts from endocardial side, and moves towards the epicardial side, while repolarisation starts from epicardial side, moves towards the endocardial side.

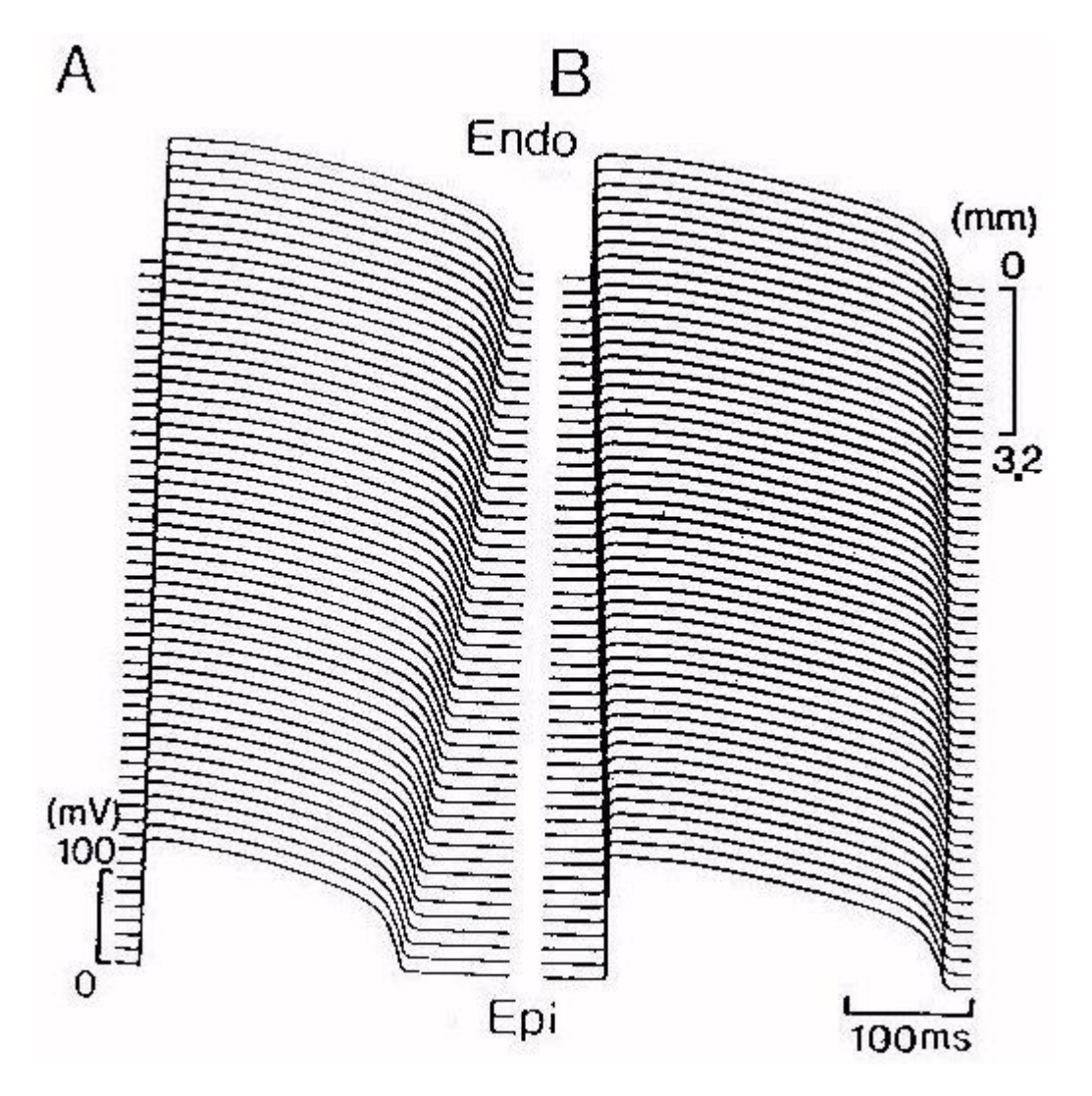


Figure 4: Computed action potentials along the length of (A) isolated cells (B) a string of guinea-pig ventricular muscle from endocardium to epicardium. A supra-threshold stimulation is applied at the endocardial end. The evoked excitation wave propagates from endocardium to epicardium. Due to the electronic interactions, the regional differences in action potential duration along the string were reduced: the measured APD_{90} were 282 ms at the end of endocardium and 271 ms at the end of epicardium, while 284 ms and 228 ms from isolated endocardial and epicardial cells.

Figure 5 illustrates quantitatively the changes of dispersion of action potential duration along the string by the electrotonic interactions between cells. In the figure, squares represent the data of isolated cells, circles represent the data of intact transmural string. Electrotonic coupling decreases the transmural dispersion of action potential duration.

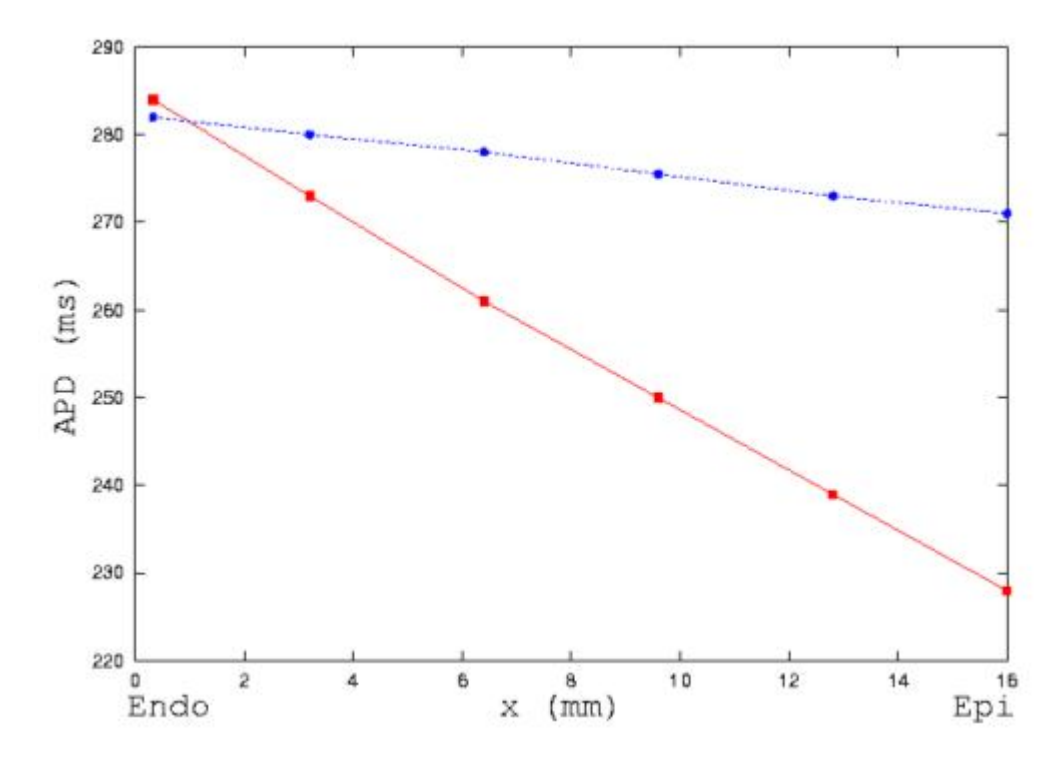


Figure 5: Computed action potential duration measured at 90 % repolarization (APD_{90}) in isolated cells (red) and a string (blue) from endocardium to epicardium in guinea-pig ventricle. Electronic interactions between cells smooth the heterogeneity of the characteristics of action potential duration.

Conclusions

Models incorporating the experimental data of regional differences on ionic current densities of guinea-pig ventricle cells have been developed. The model generated action potentials have the same regional differences as those recorded experimentally. Our modelling work supports the hypothesis that the regional differences in the electrical activities of ventricular cells are results of the regional differences in the intrinsic properties of cells through the ventricular wall. In one-dimensional model, we showed that electrotonic interactions between cells smooth the heterogeneity through the wall. It helps to explain "why the electrophysiological properties of different myocardial sites differ so markedly at the level of the isolated tissue and single cell and yet become so much more homogenous in the intact ventricle" [18]. The cell to cell coupling coefficient we used here is reasonable, with it, the conduction velocity of action potential of the string is 0.3 ms⁻¹, which is consistent with the experimental data. In the model, the computed sequence of depolarisation and repolarisation is consistent with experimental observation, which validates that our one-dimensional model is a reasonable approximation of intact transmural ventricular tissue.

Appendix

Single cell models for endo- and epicardial of guinea-pig ventricular myocytes*:

• Units

second time S millimetre mm space millivolt mV potential microfarad capacitance uF conductance uS microsiemen nA nanoampere current mMmole per litre concentration

• Independent dynamic variables

V- transmembrane voltage, mV; x_{r1} , x_{r2} , x_s - gating variables, 0 to 1; $[Na^+]_i$, $[K^+]_i$, $[Ca^{2+}]_i$ - intracellular ion concentrations, mM; $[Na^+]_0$, $[K^+]_0$, $[Ca^{2+}]_0$ - extracellular ion concentrations, mM.

• Differential equations for endo- and epicardial

$$I_{Kr} = I_{Kr} + I_{Ks} + I_{K,Na}$$

$$I_{Kr} = (G_{Kr1} + G_{Kr2})(V - E_K)/(1 + e^{(V+9)/22.4})$$

$$I_{Ks} = G_{Ks}X_s^2(V - E_{Ks})$$

$$I_{K,Na} = G_{K,Na}(V - E_K)[Na^+]_i/([Na^+]_i + k_{kna})$$

$$E_K = RT \ln([K^+]_o/[K^+]_i)/F$$

$$E_{Ks} = \frac{RT}{F} \ln \frac{[K^+]_o + P_{kna}[Na^+]_o}{[K^+]_i + P_{kna}[Na^+]_i}$$

$$Endo:$$

$$\dot{x}_{r1} = \frac{50}{1 + e^{-(V-5)/6.5}}(1 - x_{r1}) - 0.05e^{-\frac{(V-20)}{15}}x_{r1}$$

$$\dot{x}_{r2} = \frac{50}{1 + e^{-(V-5)/9}}(1 - x_{r2}) - 0.4e^{-\frac{(V-20)}{30}}x_{r2}$$

$$\dot{x}_s = \frac{14}{1 + e^{-(V-68)/24}}(1 - x_s) - e^{-\frac{V}{58}}x_s$$

$$\begin{split} \dot{x}_{r1} &= \frac{50}{1 + e^{-(v-5)/9}} (1 - x_{r1}) - 0.05e^{-\frac{(v-20)}{15}} x_{r1} \\ \dot{x}_{r2} &= \frac{50}{1 + e^{-(v-5)/9}} (1 - x_{r2}) - 0.4e^{-(\frac{v+30}{30})^3} x_{r2} \\ \dot{x}_s &= \frac{14}{1 + e^{-(v-68)/22}} (1 - x_s) - e^{-\frac{v}{58}} x_s \\ I_{NaK} &= I_{NaK \max} \frac{[K^+]_o}{[K^+]_o + k_{mk}} \frac{[Na^+]_i}{[Na^+]_i + K_{mNa}} \\ I_{NaCa} &= K_{NaCa} \frac{e^{\frac{v}{RT/F}} [Na^+]_i^3 [Ca^{2+}]_o - e^{\frac{(1-v)\frac{v}{RT/F}} [Na^+]_o^3 [Ca^{2+}]_i}}{1 + dNaCa([Na^+]_i^3 [Ca^{2+}]_o + [Na^+]_o^3 [Ca^{2+}]_i)} \end{split}$$

• Standard parameter values

^{*}Our cell models are based on the Nobel et al. model [19] with modifications as shown in the appendix.

References

- [1] Liu, D.W., Gintant, G.A. and Antzelevitch, C., "Ionic bases for electro-physiological distinctions among epicardial, mid-myocardial, and endocardial myocytes from the free wall of the canine left ventricle", Cir Res. 72: pp. 671-687, 1993.
- [2] Liu, D.W. and Antzelevitch, C., "Characteristics of the delayed rectifier current (I_{Kr} and I_{Ks}) in canine ventricular epicardial, midmyocardial, and endocardial", Cir Res. 76: pp. 351-365, 1995.
- [3] Sicouri S. and Antzelevitch, C., "Electrophysiologic characteristics of M cells in the canine left ventricular free wall", J.Cardiovasc Electrophysiol. 6: pp. 591-603, 1995.
- [4] Kimura, S., Bassett, A. L., Furukawa, T., Cuevas, J. and Myerburg, R. J., "Electrophysiological properties and responses to simulated ischemia in cat ventricular myocytes of endocardial and epicardial origin", Cir Res. 66: pp. 469-477, 1990.
- [5] Furukawa, T., Myerburg, R.J., Furukawa, N., Bassett, A.L. and Kimura, S., "Differences in transient outward currents of feline endocardial and epicardial myocytes", Cir Res. 67: pp. 1287-1291, 1990.
- [6] Fedida, D. and Giles, W.R., "Regional variations in action potentials and transient outward current in myocytes isolated from rabbit left", J. of Physiology -London 442: pp. 191-209, 1991.
- [7] Clark, R.B., Bouchard, R.A., Salinasstefanon, E., Salinasstefanon, E., Sanchezchapula, J. and Giles, W.R., "Heterogeneity of action potential waveforms and potassium currents in rat ventricle", Cardiovascular Res. 27: pp. 1795-1799, 1993.
- [8] Shipsey, S.J., Bryant, S.M. and Hart, G., "Effects of hypertrophy on regional action potential characteristics in the rat left ventricle - A cellular basis for T- wave inversion?", Circulation 96: pp. 2061-2068, 1997.
- [9] Nabauer, M., Beuckelmann, D.J., Uberfuhr, P. and Steinbeck, G., "Regional differences in current density and rate-dependent properties of the transient outward current in subepicardial and subendocardial myocytes of human left ventricle", Circulation 93: pp. 168-177, 1996.
- [10] Wettwer, E., Amos, G.J., Posival, H. and Ravens, U., "Transient outward current in human ventricular myocytes of subepicardial and subendocardial origin", Cir Res. 75: pp. 473-482, 1994.
- [11] Litovsky, S.H. and Antzelevitch, C., "Transient outward current prominent in canine ventricular epicardium but not endocardium", Cir Res. 62: pp. 116-126, 1988.
- [12] Bryant, S.M., Shipsey, S.J. and Hart, G., "Regional differences in electrical and mechanical properties of myocytes from guinea-pig hearts with mild left ventricular hypertrophy", Cardiovascular Res. 35: pp. 315-323, 1997.
- [13] Main, M.C., Bryant, S.M. and Hart, G., "Regional differences in action potential characteristics and membrane currents of guinea-pig left ventricular myocytes", Experimental Physiology 83: pp. 747-761, 1998.
- [14] Bryant, S.M., Wan, X.P., Shipsey, S.J. and Hart, G., "Regional differences in the delayed rectifier current (I_{Kr} and I_{Ks}) contribute to the differences in action potential duration in basal left ventricular myocytes in guinea-pig", Cardiovascular Res. 40: pp. 322-331, 1998.
- [15] Hirano, Y. and Hiraoka, M., "Barium-induced automatic activity in isolated ventricular myocytes from guinea-pig heart", J. of Physiology London 395: pp. 455-472, 1988.
- [16] Ryder, K.O. Bryant, S.M. and Hart, G., "Membrane current changes in left-ventricular myocytes isolated from guinea-pig heart after abdominal aortic coarctation", Cardiovascular Res. 27: pp. 1278-1287, 1993.
- [17] Coraboeuf, E., Coulombe, A., Deroubaix, E., Hatem, S. and Mercadier, J.J., "Transient outward potassium current and repolarization of cardiac cells", Bulletin de l Academie nationale de Medecine 182: pp. 325-335, 1998.
- [18] Anyukhovsky, E.P., Sosunov, E.A., Gainulin, R.z. and Rosen, M.R., "The controversial M cell", J. Cardiovascular Electrophysiology 10: pp. 244-260, 1999.
- [19] Noble, D., Varghese, A., Kohl, P. and Noble, P., "Improved guinea-pig ventricular cell model incorporating a diadic space, I_{Kr} and I_{Ks} , and length- and tension- dependent processes", Canada J. of Cardiology 14: pp. 123-134, 1998.
- [20] Oxford cardiac electrophysiology group. Oxsoft HEART version 4.8 manual; Oxford: Oxsoft, 1997.
- [21] Bjornstad, H., Tande, P.M., Lathrop, D.A. and Refsum, H. "Effects of temperature on cycle length- dependent changes and restitution of action potential duration in guinea-pig ventricular muscle", Cardiovascular Res. 27: 946-950, 1993.
- [22] Boyett, M.R. and Fedida, D. "Changes in the electrical activity of dog cardiac Purkinje fiber at high rates", J. Physiol. 350: pp. 361-391,1984.

